IRSTI 38.31.15
Article

Integrated facies analysis, paleoecology, and diagenetic evolution of the Eocene–Oligocene succession, northern Bahariya depression, Egypt: sequence stratigraphic perspectives

Nada A. Ayoub[1], Sayed M. Ahmed[1], Rifaat A. Osman[1], Mervat S. Hassan[2], Emad S. Sallam[1]*

[1]Benha University, Benha, Egypt; n.ayoub58969@fsc.bu.edu.eg, sayed.ahmed@fsc.bu.edu.eg, r.othman@fsc.bu.edu.eg
[2]Central Metallurgical Research Development Institute, Cairo, Egypt; mervat_hassan45@yahoo.com
*Correspondence: emad.salam@fsc.bu.edu.eg

Abstract. This study describes the depositional facies, paleoecological, sequence, and diagenetic features of the Eocene–Oligocene succession exposed in northern Bahariya Depression, Western Desert, Egypt. This Eocene–Oligocene succession is composed of five stratigraphic units, from base to top, the Naqb (early Eocene), Qazzun (middle Eocene), and El-Hamra (middle-late Eocene) formations, followed by the Radwan (early Oligocene) and El-Ris (late Oligocene-Miocene?) formations. Several miscellaneous larger benthic foraminiferal and macrofaunal assemblages were identified from the studied Eocene rock units and interpreted ecologically. Analyses of litho-, bio-, and microfacies resulted in the recognition six major facies associations that record a range from peritidal flats to restricted and outer lagoons, and reefal environments of the Eocene rocks, to fluvial and shallow lacustrine terresteiral environments of the Oligocene rocks. The most common diagenetic features recorded in the examined rocks likely resulted from cementation, dolomitization, silicification, glauconitization, and iron replacement.
The studied Eocene-Oligocene succession is comprised of two major systems tracts, a transgressive systems tract at the bottom, followed by a regressive systems tract at the top. The change of depositional trend from a transgressive to a regressive mode essentially developed in response to the progressive decrease in accommodation space and the increase of sediment supply.

Keywords: Depositional environments; paleoecology; diagenesis; sequence stratigraphy; Eocene; Oligocene; Bahariya depression.

Citation: Ayoub, N.A., Ahmed, S.M., Osman, R.A., Hassan, M.S., Sallam, E.S. (2025). Integraged facies analysis, paleoecology, and diagenetic evolution of the Eocene-Oligocene succession, northern Bahaariya depression, Egypt: sequence stratigraphic perspectives. Journal of Ecology and Sustainability, 153(1), 20-40. https://doi.org/10.32523/59fsh138

Academic Editor:
A. Zandybay

Received: 03.12.2025
Revised: 09.12.2025
Accepted: 12.12.2025
Published: 30.12.2025

1. Introduction

Sedimentary facies analysis is a crucial tool for understanding the depositional evolution of sedimentary basins. By analyzing the characteristics of sedimentary rocks, such as lithology, texture, and fossil content, it is possible to reconstruct the depositional processes that shaped the basin (Wilson, 1975; Flügel, 2010). Sequence stratigraphy and diagenetic evolution are also essential for understing the geological history of a sedimentary basin, as they provide insights into the tectonic, sea-level, and climatic controls on sedimentation and rock formation

(Tucker, 1981; Tucker and Wright, 1990; Catuneanu, 2006; Catuneanu et al., 2011).

The Eocene–Oligocene rocks exposed in the northern Bahariya Depression have been characterized in several studies (El Akkad and Issawi, 1963; Said and Issawi, 1964; El Bassyony, 1980; Moustafa et al., 2003; Boukhary et al., 2011; Afify et al., 2016; Ayoub et al., 2025a, b and references therein). These studies dealt mainly with the litho- and biostratigraphy and structural setting, as well as the genesis of the Eocene-hosted ooidal ironstones. Khalifa and Maashal (2023) and Assal et al. (2024) have made a significant contribution to the sedimentology of the middle-upper Eocene rocks in this area. However, sequence stratigraphy and diagenetic evolution of these rocks have not been fully achieved. Therefore, the present study aims to: 1) analyze the sedimentary facies of the Eocene–Oligocene rocks exposed in northern Bahariya Depression, and reconstruct their depositional environments, as well as to define the ecological characteristics of their macrofaunal assembalges, 2) investigate the diagenetic features of the studied Eocene–Oligocene rocks, and 3) establish a transgressive–regressive (T–R) sequence stratigraphic framework for the studied Eocene–Oligocene succession, and identify the key controls on sedimentation.

Geological setting

The Bahariya Depression is a prominent, roughly oval-shaped topographic low (~120 km long, 40-50 km wide) situated in the Western Desert of Egypt, approximately 370 km southwest of Cairo. It occupies a structural basin developed during the Late Cretaceous–early Cenozoic tectonic activity associated with the opening of the Neotethys and the subsequent Syrian-Arc-Fold-System, which created a series of NE-SW trending folds and fault systems that control its morphology (Said, 1962; Said and Issawi, 1964; Moustafa et al., 2003). The depression is made up of a thick succession of Upper Cretaceous to Paleogene sediments that unconformably overlie the Precambrian basement rocks (Figure 1). The Eocene–Oligocene interval, of particular interest, comprises a mixed carbonate–siliciclastic sequence that records a transition from marginal-marine shelf environments (the lower Eocene Naqb Formation) to more restricted lagoonal and peritidal settings of the middle Eocene Qazzun Formation, followed by the middle-upper Eocene marginal-marine, reefal carbonates and siliciclastics of the El-Hamra Formation (Ayoub et al., 2025a, b). These rock units are well-exposed along the northern plateau of the Bahariya Depression, where they form a gently north-dipping homoclinal ramp (Assal et al., 2024; Ayoub et al., 2025a, b). The lower-upper Eocene succession is overlain disconformably by the Oligocene fluviatile sandstones of the Radwan Formation, followed by lacustrine carbonates of the El-Ris Formation (late Oligocene-Miocene?). The interplay of eustatic sea-level fluctuations, regional subsidence, and episodic uplift during the Eocene–Oligocene shaped the depositional architecture, creating a mosaic of facies belts that range from peritidal flats and lagoons to reefal margins and shallow-marine platforms (El Akkad and Isswai, 1963; Said and Issawi, 1963).

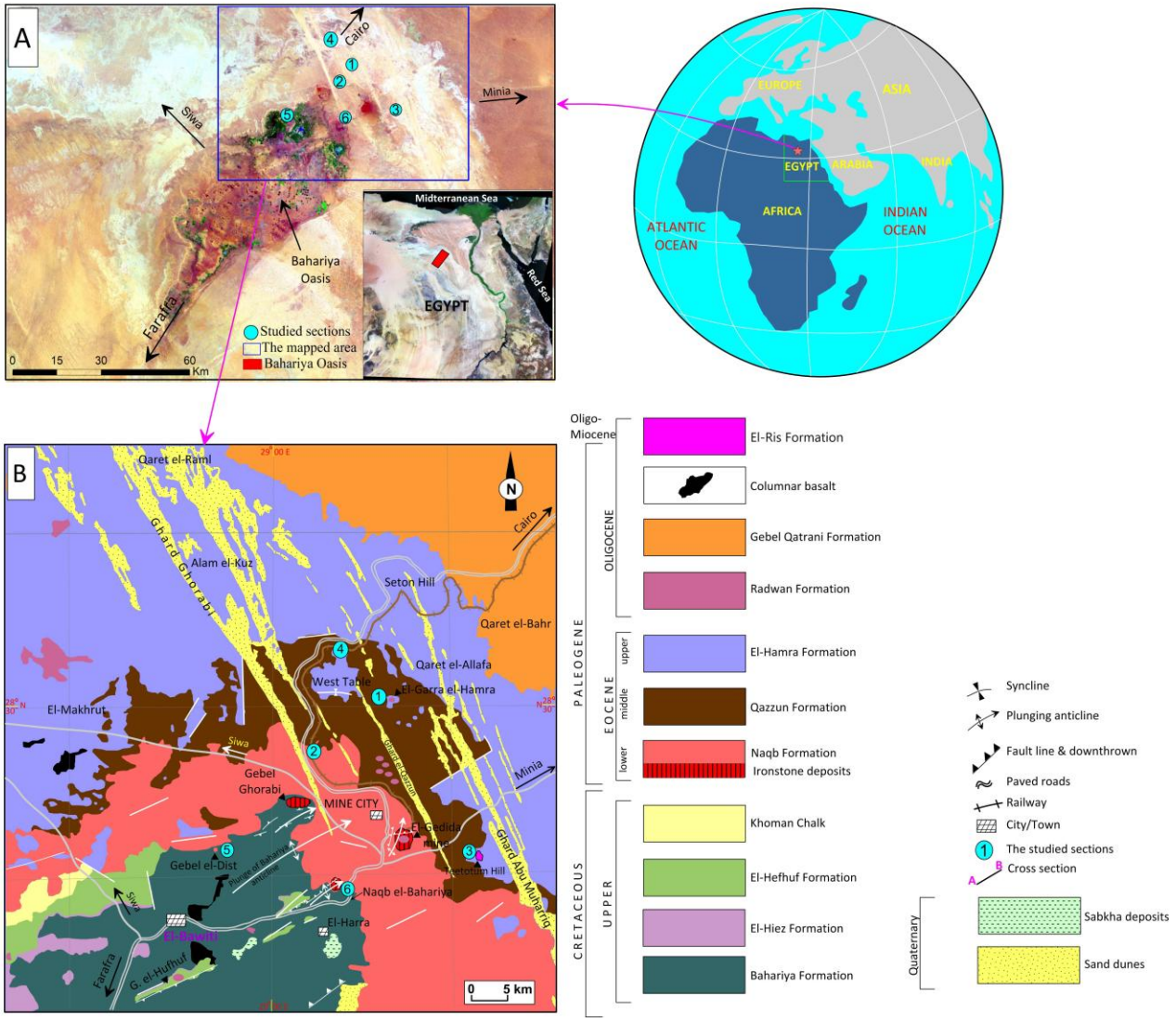

Figure 1. A) ETM+ Lsat image of the Bahariya Depression showing the locations of the studied Eocene-Oligocene sections. B) Geological map showing the stratigraphic units exposed in the northern part of the Bahariya Depression (El Akkad and Issawi, 1963)

2. Materials and methods

A comprehensive workflow was employed to characterize the depositional facies, diagenetic, and paleoecological attributes of the studied Eocene–Oligocene succession exposed in the northern plateau of the Bahariya Depression, Egypt. Fieldwork involved detailed logging of six stratigraphic sections, documenting lithology, sedimentary structures, fossil content, and bedding geometry (Figure 2). Some representative hand-specimens (n = 65) were collected for petrographic investigation. Thin-sections were prepared from different lithofacies types and examined under a polarizing microscope to identify microfacies, allochems, and diagenetic features. Limestone microfacies classification followed Dunham (1962) scheme. A subset of carbonate thin-sections was etched and stained with Alizarin Red-S dye following the modified staining technique of Dickson (1965) in order to distinguish between calcite and dolomite. Through this method, non-ferroan calcite and aragonite turn pink to reddish-brown colours, while non-ferroan dolomite remains colourless. Sandstone textures are described following the classification schemes of Pettijohn et al. (1973). Through this method, non-ferroan calcite and aragonite turn pink to reddish-brown colours, while non-ferroan dolomite remains colourless. The most characteristic microscopic textures and skeletal and non-skeletal constituents were photographed using an integrated Olympus LC20 digital camera attached to an Olympus BX51 polarizing microscope.

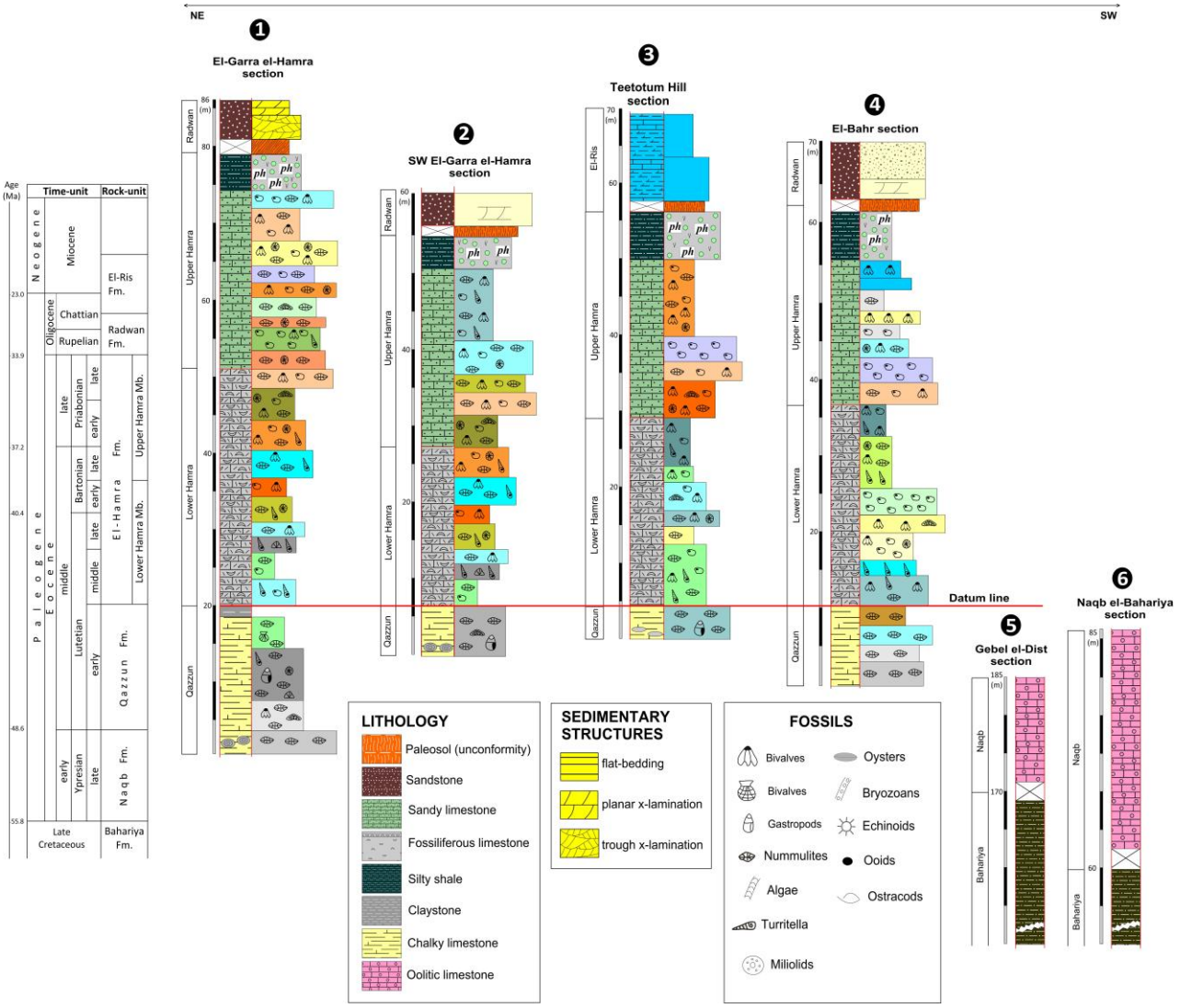

Figure 2. Sedimentary logs of the studied Eocene–Oligocene succession in the study area, showing the distribution and characteristic constituents of the identified facies associations

3. Results

3.1. Faunal assemblages and paleoecology

The lower–middle Eocene rocks exposed in the northern Bahariya Depression yield abundant larger benthic foraminifera, particularly nummulites, assilines, operculines, orthophragmines, and orbitolites, in addition to the abundant presence of benthic macrofossils of bivalves, gastropods, cephalopods, echinoids and bryozoans. These benthic fauna were predominantly inhabited in the inner neritic, near-coast tide-dominated zone (<100 m depth), which is characterized by warm water with normal to restricted salinity, and sluggish to open water circulation necessary for transferring nutrients to the lagoons and reefs (Flügel, 2004). Apparently, there were significant upward paleoecological shifts across the lower–upper Eocene succession triggered by variation in neritic siliciclastic inflow due to tectonic and climatic instability.

In this study, four local larger benthic foraminiferal total range zones were identified from the lower–upper Eocene rocks (Figure 3). These zones correspond to the regional shallow benthic foraminiferal zones (SBZ12 through SBZ19) of Serra-Kiel et al. (1998) established throughout the Tethyan carbonate platforms. The identified LBFs total range zones in the studied Eocene succession are arranged from base to top, as follows: (1) *Orbitolites complanatus* Total Range Zone

(late Ypresian = SBZ12), (2) *Nummulites praelorioli* Total Range Zone (late Ypresian–early Lutetian = SBZ12 & SBZ13), (3) *Nummulites gizehensis–Nummulites beaumonti* Interval Zone (middle Lutetian–early Bartonian = SB14–SBZ17), and (4) *Nummulites contortus-striatus* Total Range Zone (late Bartonian–Priabonian = SBZ18 & SBZ19).

Benthic macrofossils (e.g., bivalves, gastropods, bryozoans and echinoids) collected from the studied Eocene rocks provide significant information about the palaeoecological and palaeoenvironmental conditions that prevailed during their deposition (Ayoub et al., 2025a, b). Five distinctive macrofaunal assemblages were identified from the studied lower–upper Eocene exposures in northern Bahariya Depression. These faunal assemblages were identified and interpreted in terms of palaeoecological conditions (Figure 3).

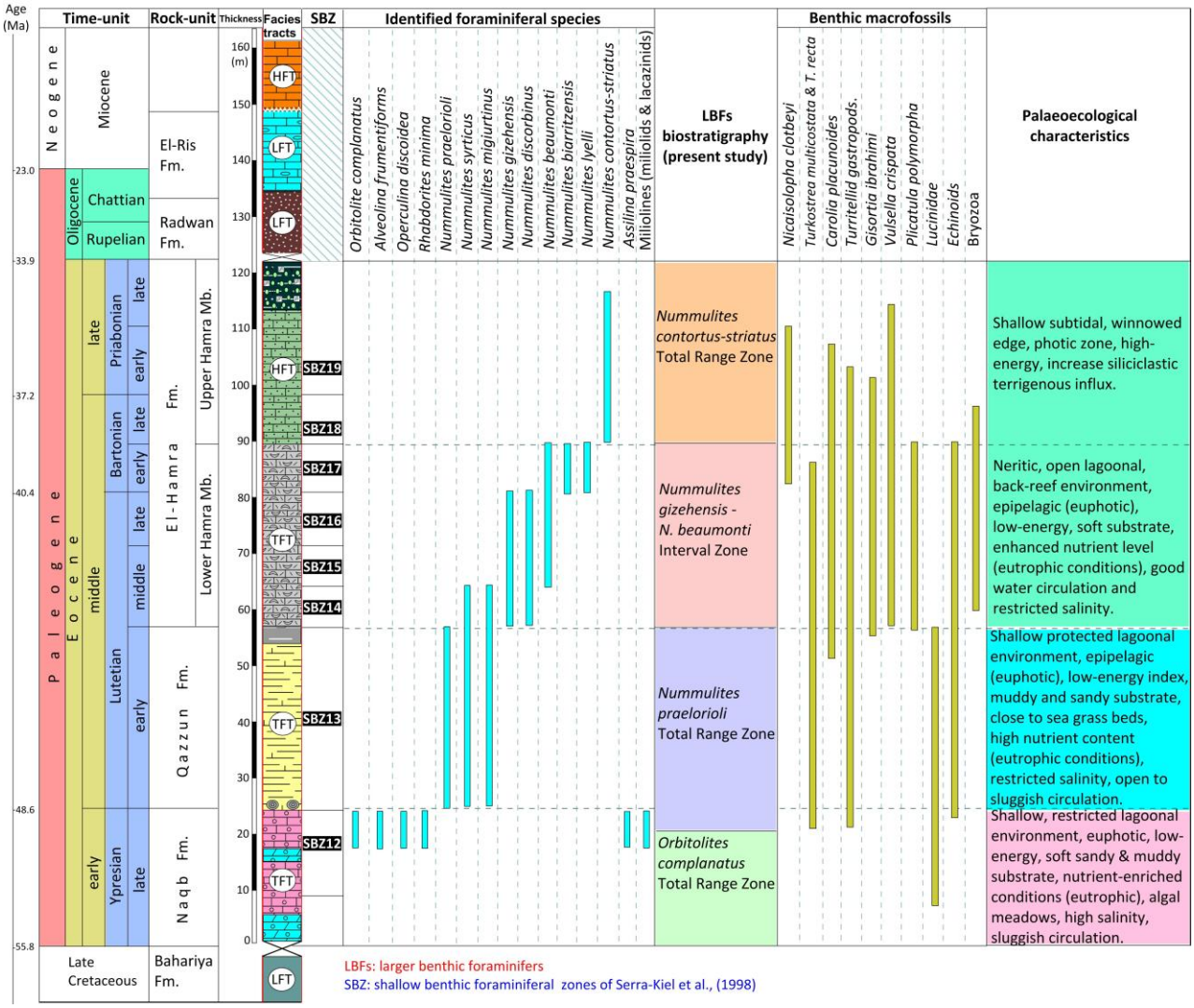

Figure 3. Biostratigraphic chart demonstrating the larger benthic foraminiferal zones with respect to the shallow larger benthic foraminiferal zones (SBZ) of Serra-Kiel et al. (1998) and other benthic macrofossils identified from the lower–upper Eocene rock units exposed in the studied area, with their palaeoecological characteristics (after Ayoub et al., 2025a, b)

3.2. Facies associations and depositional environments

The Eocene–Oligocene succession in the northern plateau of the Bahariya Depression exhibits a well-defined spectrum of facies associations that record a range from marginal-marine peritidal flats to inner-restricted lagoons, outer lagoons, and reefal environments, to fluviatile and shallow lacustrines, as documented by Assal et al. (2024) and Ayoub et al. (2025a, b). Facies analysis of the

studied Eocence–Oligocene succession revealed nineteen microfacies types that have been grouped into six facies associations, and summarized in Table 1.

Table 1. Summary of microfacies types, facies associations and depositional environments of the studied Eocene–Oligocene rocks exposed in the northern plateau of the Bahariya Depression

Facies Associations /microfacies types	Textural constituents	Depositional environments & paleoecology
FA1: Peritidal flat facies association		
mf1: Lime-mudstone	0.5–2.0 m-thick, earthy-gray to grayish-brown homogenous micrite with few disseminated quartz grains and bioclastic particles.	Low-energy tidal flat (FZ8) and arid evaporitic coastline (FZ9 of Wilson's model (1975)) environments reflecting a short-term of sea-level fall (Tucker and Wright, 1990). It is consistent with the SMF23 of (Flügel, 2004). Dolomitization most probably took place in the early diagenesis, and is related mostly to hypersaline brines of a tidal flat-inner lagoon setting (Keheila and El-Ayyat, 1990, 1992; Sallam et al., 2015a,b; Sinanoğlu et al., 2018; Sallam et al., 2018, 2022).
mf2: Dolomicrite	Anhedral to subhedral dolomite rhombs ranging in size from 10 to 15 μm. Hypidiotopic fabric with equigranular texture. Unzoned crystals showing cloudy cores and clear outer peripheries.	
mf3: Foraminiferal dolomicrite	Similar to the above-described mf2, with few skeletal particles, commonly larger benthic foraminifera and bioclastics, which partially/fully dolomitized.	
mf4: Sandy bioclastic rudstone	It consists mainly of oyster shells, gastropods and minor nummulites showing aggrading neomorphism and embedded in a micritic matrix.	Neritic, littoral-sublittoral, high to moderate-energy subtidal and intertidal zones (FZ7 & FZ8 of Wilson's model (1975)).
mf5: Laminated-glauconitic-anhydritic-sandy shale	Laminated glauconitic-gypseous-sandy shale with few small scale cross-bedded sandstone, siltstone and marlstone intercalations. Glauconite grains show yellowish-green to dark-green, rounded to subrounded, fine to medium-grained (100–350 μm), well-sorted to poorly-sorted pellets embedded in a dark ferruginous clayey matrix. Glauconite pellets also fill foraminiferal and fossil shells. Anhydrite crystal laths were also common.	Slow sedimentation rates in a reduced shallow-water nearshore tidal flat to restricted inner ramp lagoonal environments (FZ7–9 of Wilson's model (1975)), influenced by wave energy, and continuously received high influx of terrigenous siliciclastic sediments.
FA2: Open lagoonal–restricted bays facies association		
mf6: Miliolidal foraminiferal wacke- to packstones	It is made up of abundant larger (*Orbitolites*, *Alveolines*) and miliolidal foraminifera (*Pseudolacazines*, *Biloculina*, *Quincloculina*, *Rhabdorites*), with a few occurrence of calcareous algae, crinoids, and echinoid spines; all are embedded in a microsparitic matrix.	Low-energy neritic, restricted inner ramp lagoonal environment (FZ8 of Wilson's model (1975)), epipelagic euphotic, under a sluggish to open circulation and high saline shallow-water and eutrophic (high nutrient level) conditions (Wilson, 1975; Flügel, 2010).
mf7: Algal foraminiferal wacke- to packstones	This microfacies consists of nummulites, algal debris and small miliolidal foraminifera that are embedded in a microsparitic matrix. Some bioclasts exhibit micritization and/or micrite coatings and patchy neomorphism is present in the micritic matrix.	
mf8: Foraminiferal wackestones	The mf8 consists of floated foraminiferal species distributed within a microsparitic to	

	micritic matrix.	
mf9: Sandy bioturbated bioclastic wacke- to packstones	It is composed of molluscan shell fragments, bryozoan debris and few miliolidal foraminifera that are embedded in a micritic matrix.	
mf10: Ferruginous oolitic–pisolitic wacke- to packstones	Hematitic and goethitic spherical to irregular-shaped curved grains of ooids (less than 2 mm in diameter) and pisoids (larger-sized) with quartz nuclei and a cortex of concentric hematite/goethite laminae that are cemented by ferroan calcite. Bioclastics are also impregnated by hematite/goethite.	Low-energy, proximal lagoons and restricted bays, with sluggish water (El Akkad and Issawi, 1963; Said and Issawi, 1964).
FA3: Barrier shoal facies association		
mf11, 12: Foraminiferal ooidal/pelloidal wacke- to packstones	Coated grains of ooids/pisoids, and pelloids and miliolid foraminmiferal shells embedded in a microsparitic matrix. Some bioclasts enveloped by micrite coatings, others show aggrading neomorphism and filled with sparite cement.	Winnowed platform margin–restricted lagoonal environments (FZ6 of Wilson's model (1975)) with a normal marine salinity, high-energy, open circulation and constant wave action (Wilson, 1975; Flügel, 2004).
FA4: Platform margin reefal facies association		
mf13: Nummulitic wacke-, pack- to grainstones	It consists of bioclasts mainly nummulites, assilina and operculines with minor oyster shell debris and subordinate ratio of quartz grains, embedded in a micritic matrix, partly microsparitic.	Tropical to subtropical, outer open lagoon–platform margin reefs with photic, warm, open to moderate current circulation, and high nutrient levels (eutrophic) in the platform interior–open marine (FZ7 and FZ9 of Wilson's model (1975)).
mf14: Burrowed bioclastic rudstones	It is composed of bioclasts of oyster shell fragments, gastropods and a few larger benthic foraminifera embedded in microsparitic matrix.	
mf15: Echinoidal wackestones	It consists of echinoid spines, crinoids and other bioclastic shell fragments.	
mf16: Bryozoan framestones	It consists of bryozoan fragments, in addition to larger foraminifers, bioclasts and quartz grains embedded in a micritic, partly sparitic matrix.	
FA5: Fluvial channel facies association		
mf17: Quartz-arenite and sub-litharenite	It is made up mainly of monocrystalline quartz, with subordinate lithic fragments and very rare feldspar grains. It shows a grain-supported fabric, and subangular to well-rounded, low sphericity, and poorly to moderately-sorted texture. Most monocrystalline quartz grains show straight extinction, and few grains show undulose extinction.	Fluvial channels, with characteristic features of sinuous, high-energy, meandering-style paleorivers.
FA6: Shallow lacustrine facies association		
mf18: Calcrete	It consists of fossiliferous lime-mudstone to wackestone and microspary calcite including dispersed quartz grains and delicate small fossils commonly of two-valved, oval to elongate ostracods, gastropods, and charophytes and stromatolites.	Alkaline–Mg^{2+} enriched shallow lacustrine environment in vadose and vadose-phreatic zones, under evaporitic and palustrine conditions (FZ10 of Wilson's model (1975)).
mf19: Dolocrete	It consists of dolomicritic including	

	dispersed quartz grains with lense-shaped, elongated, rounded to oval arthropod microfossils of ostracods and shell debris filled with sparitic cement. The dolomicrite consists of microcrystalline dolomite rhombs (5–15 μm) showing equigranular and idiotopic textures.	

3.3. Diagenetic features

Sediment diagenesis specifically signifies to any physical and/or chemical modifications to the sediment after its deposition. These modifications most often cause a marked change in the original texture and framework of the sediment (Tucker and Wright, 1990). In the following paragraphs, we provide a detailed description and interpretation of the most common diagenetic features observed in the studied carbonate and sandstone facies. The studied Eocene–Oligocene rocks exhibit a variety of diagenetic features resulted from compaction, cementation, recrystallization (neomorphism), replacement (including dolomitization, silicification and iron replacement), dissolution, and glauconitization.

3.3.1. Compaction and cementation

Mechanical compaction is well-observed through the fracturing of many pelecypods foraminiferal shells in the studied Eocene microfacies (Figure 4A). Chemical compaction is also indicated by stylolitic contacts between many quartz grains of the Radwan sandstones. Cement materials in the recognized limestone facies vary from micrite and microsparite to large poikilotopic drusy calcite crystals (Figure 4B), whereas in the sandstone clastic facies, quartz overgrowths (Figure 4C), calcite and goethite are common. The origin of silica for quartz overgrowths cementation is most often attributed to pressure solution, in which pore solutions become enriched with respect to silica, which is then reprecipitated as overgrowths around the parent quartz grains when supersaturation is attained. Other probable sources for silica overgrowths might be attributed to ascending hydrothermal solutions or to the dissolution of silica dust of wind abrasion and other silicates (Waugh, 1970), or dissolution of feldspars, amphiboles and pyroxenes during the early stages of daigenesis (McBride, 1989).

3.3.2. Micritization

Micritization is observed in pelecypod and foraminiferal shells, which are subjected to partial and/or full micritization. Some nummilte ghosts seen in some thin-sections are most probably attributed to the full micritization of their shells in the early stages of diagenesis (Figure 4D). Micritization often occur due to shell abrasion by microbial activity or micro-borings of endolithic dasyclad algae in shallow-water photic environments forming micrite envelopes around biogenic particles (Figure 4D) (Folk, 1962; Bathurst, 1975; Tucker, 1981). It can also originates through aragonite transformation into micrite (Fischer et al., 1967). Aggrading neomorphism occurs largely in lime-mudstone (calcilutites) and wackestone microfacies of the El-Hamra Formation, and is indicated by the patchy development of microspars and pseudospars in the micrite groundmass. Aggrading neomorphism most likely promoted through the gradual removal of Mg^{2+} from micritic limestone by meteoric water influxes or adsorption in clays that letting micrite to increase in size, forming microsparite and sparry calcite eventually (Folk, 1974; Longman, 1977). Recrystallization is also a common diagenetic feature recorded in the bioclastic–nummulitic packstone and grainstone microfacies of the investigated Eocene microfacies. This can be distinguished where the originally aragonitic shells are recrystallized to sparry calcite (Figure 4E). Fossil dissolution was also discerned in the studied Eocene microfacies, producing moldic vuggy porosity (Figure 4F). Karstification occurred in the Eocene limestones has also led to frequently development of irregular cavities of variable sizes from tiny voids to large caves filled with well-developed calcite crystals (Figure 4G).

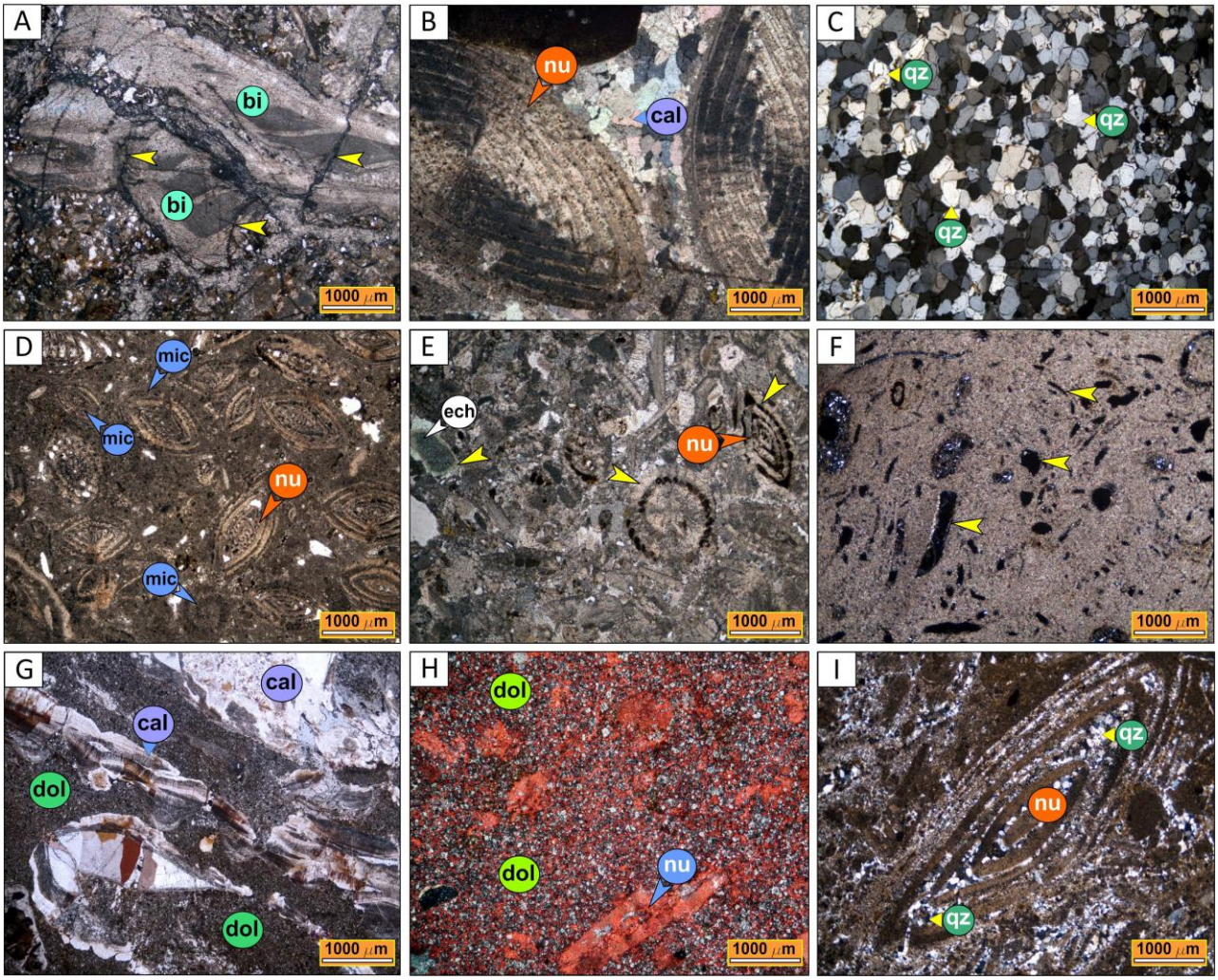

Figure 4. Thin-section photomicrographs of a variety of diagenetic features observed in the studied Eocene–Oligocene rocks. A) Fracturing shifting (yellow arrows) in bivalve shell fragments (bi), pointing out to intense mechanical compaction. Sandy oyster rudstone, Lower Hamra Member. B) Bioclast-nummulite (nu) particles cemented by large poikilotopic calcite (cal) crystals, Qazzun Formation. C) Sandstone cementation by quartz overgrowths (qz) exhibiting an optical continuity with the parent quartz grains. Crystal faces have developed in places, Radwan Formation. D) Micrite envelops (mic) around nummulite (nu) shells. Note, some bioclasts show full micritization clearly appeared in nummulite ghosts. Nummulitic packstone microfacies, Qazzun Formation. E) Partial recrystallization of nummulite (nu) and echinoid (ech) tests (yellow arrows) where aragonite is recrystallized to microsparry calcite, bioclastic-nummulitic packstone microfacies, Lower Hamra Member. F) Moldic vuggy porosity (yellow arrows) produced by fossil dissolution, Naqb Formation. G) Well-developed calcite crystals (cal) filling cavities and fissures (speleothems) within the Qazzun dolostone. The groundmass consists of equigranular dolomicrite (dol) (1–5 µm rhombic crystals). H) Stained thin-section showing partial/fully dolomitization of nummulitic wackestone of the Qazzun Formation, XPL. I) Bioclast particles and nummulite tests (nu) showing partial silicification by authigenic fine-grained quartz (qz), nummulitic packstone microfacies, Naqb Formation. Note: all photomicrographs were taken with crossed polars (XPL) and magnification X 2.5

3.3.3. Dolomitization

Dolomitization is clearly observed in the foraminiferal-bioclastic dolomicritic limestones of the lower-middle Eocene Naqb and Qazzun formations. The dolomicrite (1–5 micron-sized rhombs) forms an equigranular fabric. There is additional evidence in the form of partly dolomitized

nummulites and other biogenic particles (Figure 4H), indicating replacement during early diagenesis. Dolomitization is interpreted to be occurred by seepage–reflux in an evaporitic, supratidal environment with high Mg/Ca ratio (Adams and Rhodes, 1960). Dolomite formed in such evaporitic–supratidal environments denotes most often to a major regressive phase.

3.3.4. Silicification

Silicification, including chertification, commonly occurred within the limestone of the middle Eocene Qazzun Formation, where it contains abundant large-sized (0.5–1.0 m in diameter), spherical-shaped, hard siliceous fossiliferous limestone concretions and smaller-sized (8–20 cm in diameter) elongated and irregular-shaped chert nodules. The latter consists mainly of crypto-, and microcrystalline quartz, a few microns across. Nodular cherts in limestones are probably for the most part penecontemporaneous, formed just after deposition in shallow-marine shelf environements (Laschet, 1984). The silica that forms these cherts is possibly sourced from organically precipitated silica from sponge spicules, diatoms, and radiolarians preserved in the parent host sediments. However, some authors favor the hypothesis that most cherts, apart from those including distinctly organic, are replacements of pre-existing rocks (Peterson and von der Borch 1965; Eugster, 1969; Knauth, 1979). The inspected nodular chert is, thus, presumed to be diagenetic in origin, being partially replaced by the Qazzun limestones during the early stages diagenesis. Another important source of this silica is almost certainly the windblown sand grains input into the shallow-marine carbonate shelf. The large-sized spherical-shaped limestone concretions marking the boundary surface between the Naqb and Qazzun formations were also exteremly affected by silicification process, by which almost all bioclastic particles and other nummulite tests are partially/completely replaced by authigenic detrital fine-grained quartz (Figure 4I) that made these concretions siliceous in lithology and more harder to resist differential weathering than their the host limestonesc (Plyusnina et al., 2016; Al-Dhwadi and Sallam, 2019; Sallam and Ruban, 2019), so that these siliceous concretions were individually detached above the boundary surface forming what is known as "melon-fields".

3.3.5. Iron replacement

Iron replacement is a common diagenetic feature, where the lower part of the Naqb Formation is locally replaced by oolitic–pisolitic ironstones. There has been much discussion on the origin of the Bahariya ironstones, and several hypotheses have been postulated to explain the source of the iron into the Bahariya basin. Among these hypotheses are that: i) iron-oxides being formed by direct precipitation in lacustrine or shallow lagoonal environments, and then replaced the underlying lower Eocene carbonate rocks (Ball and Beadnell, 1903; Attia, 1950; Gheith, 1955; El-Shazly, 1962; El Akkad and Issawi, 1963), ii) metasomatism caused by ascending hydrothermal fluids (Nakhla, 1961; Basta and Amer, 1969; El Sharkawi et al., 1984), iii) volcanic eruptions (Tosson and Saad, 1974), iv) lateritization karstification (El Aref and Lotfy, 1985; El Aref et al., 2006; Salama et al., 2015), and v) deep weathering of the overlying upper Eocene glaucony sediments (Dabous, 2002; Baioumy and Hassan, 2004; Baioumy et al., 2013).

In the present study, we advocate a detrital origin for the Bahariya ironstones, by which ironstone crusts (5.0–15 cm-thick) dominated the lower Cenomanian Bahariya Formation were leached out through extensive wet tropical weathering deposited alongside with the Naqb limestone in some proximal restricted lagoons formed throughout the northern limestone plateau of the Bahariya Depression during the gradual regression, and then the iron oxides concentrated in these basins eventually replaced the surrounding Eocene fossiliferous limestone (Figure 5A) (Attia, 1950; Gheith, 1955; El Akkad and Issawi, 1963; Said and Issawi, 1964). Evidence is the frequent occurrence of ferricretes of diagenetic origin in the lower Cenomanian Bahariya Formation, which formed the core of the Bahariya anticline (Tanner and Khalifa, 2010). Further evidence is that almost all ooids, nummulites and other biogenic particles within the lower Naqb limestones have been partly or fully replaced by iron oxides during the early stage of diagenesis (Figures 5B, C). However, further specific investigations on the genesis of these ironstones, supplemented by more evidence, are required to ascertain this assumption. The sandstone of the Oligocene Radwan Formation was also affected by ferrugination and pigmentation, where almost all quartz grains are

outlined by iron-oxides coatings (Figure 5D), giving a reddish-black appearance to the sandstone. This is most probably attributed to hydrothermal solutions emanated through the highly magmatic activity initiated in the Bahariya region during the late Oligocene–early Miocene.

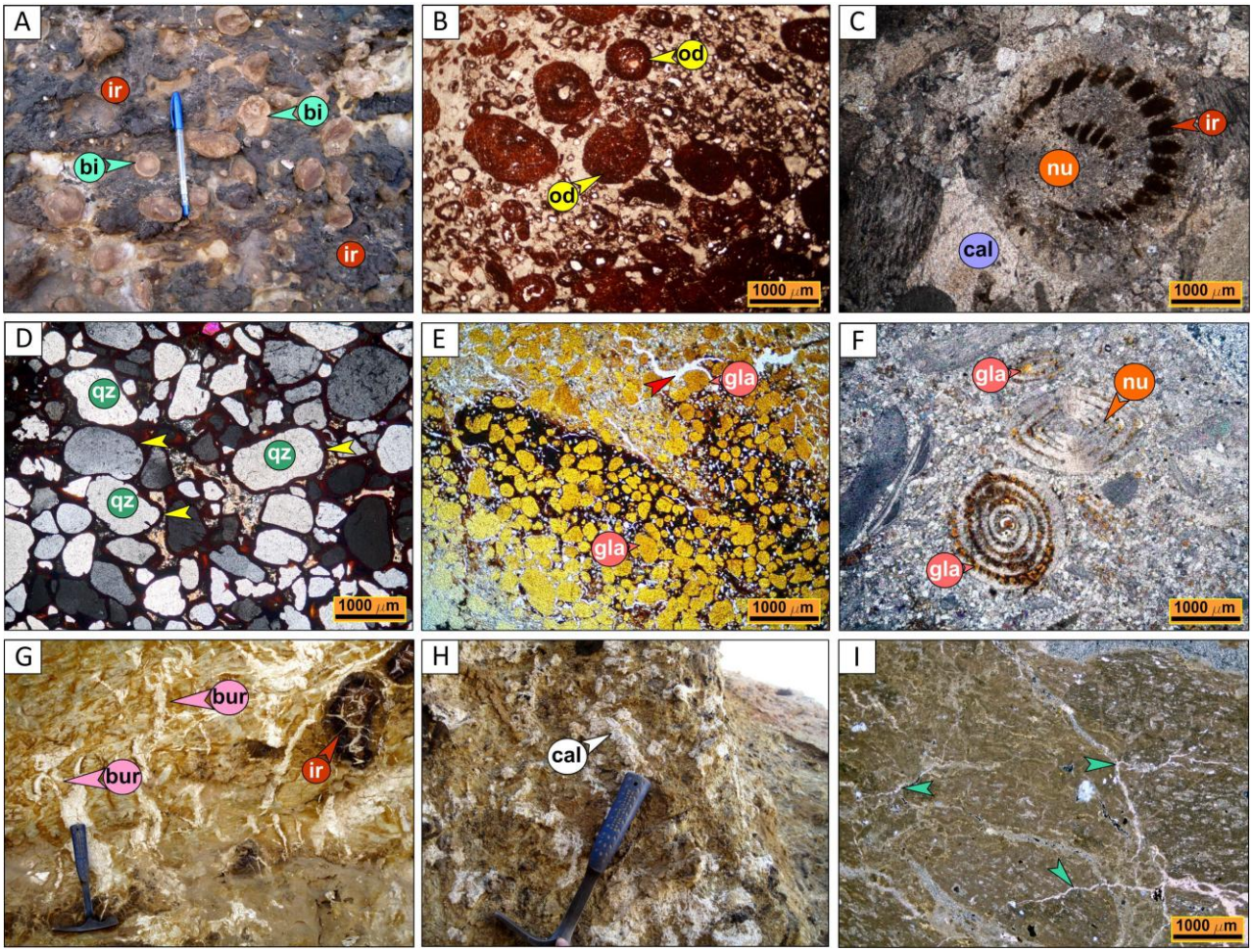

Figure 5. Microscopic field photographs showing some diagenetic features observed in the studied Eocene–Oligocene rocks. A) Field photograph showing the fossiliferous limestone in the lower part of the Naqb Formation impregnated by iron oxide (ir) material that locally replaced the limestone. Bioclastic fossils (bi) are also impregnated by iron material, El-Harra section. B) Hematite-impregnated ooids (od). Some ooids have quartz nuclei and a ruby red-colored hematitic cortex, Naqb Formation. C) Nummulite particles filled partly by iron oxides (ir), and cemented by large poikilotopic calcite (cal), Naqb Formation. D) Black iron-oxide coatings (yellow arrows) around the monocrystalline quartz (qz) grains of the Radwan sandstone, Gebel El-Garra El-Hamra section. E) Greenish-yellow, moderately-sorted, rounded, medium-grained glauconite (gla) showing some pedogenic rootlets that filled by microsparry calcite (red arrow). F) Glauconite pellets (gla) filling nummulite (nu) and fossil shells. G) Field photograph showing glauconitic sandy shale sediments with pedogenic features of color mottling, iron oncoids (ir), bioturbation (bur), and rootless as a result of subaerial exposure. The hammer for scale is 26 cm long. H) Field photograph showing greenish-colored glauconitic shale containing whitish-colored caliche (cal) nodules due to subaerial exposure. I) Calcrete limestone of the El-Ris Formation exhibiting pedogenic branched rootlets (green arrows) filled with microsparry calcite. Note: all photomicrographs were taken with crossed polars (XPL) magnification X 2.5

3.3.6. Glauconitization

Glauconitization is substantiated by the abundant occurrence of glauconite in the uppermost part of the El-Hamra Formation. Such an occurrence represents a good indicator of the stratigraphic

depositional disconformity at the latest Eocene that promoted glauconitization through increasing concentration of potassium (Odin and Fullagar, 1988; Amorosi, 1995). The glauconitic sandy shale in this rock unit constitutes a condensed section, assuming about 10 m-thick, covered by ~4.0 m-thick bluish-gray, calcareous grits and gypsum layers at the El-Harra ironstone mine, and decreases to about 10 m-thick at El-Gedida mines. Petrographically, glauconite grains appear as yellowish-green to dark-green, rounded to subrounded, fine to medium-grained (100–350μm), well-sorted to poorly-sorted pellets embedded in a dark ferruginous clayey matrix (Figure 5E). Glauconite pellets also fill foraminiferal and fossil shells (Figure 5F).

The given glaucony facies characteristics and geochemical data indicate slow sedimentation rates in a reducing shallow-water tidal flat to nearshore lagoonal environment at water depth less than 50 m that was strongly influenced by wave energy and was continuously receiving high influx of terrigenous siliciclastic sediments (Bell and Goodell, 1967; MacRae, 1972). Mesaed and Suror (1999, 2000) and El Habaak et al. (2016) suggested a parautochthonous origin for the upper Eocene glaucony facies in the studied Bahariya region, where substrate siliciclastic, K-poor, Fe-smectite precursors were progressively transformed into micaeous, K- Fe^{3+}–rich glauconite through the formation of glauconite–smectite intermediates at the sediment–seawater interface during the early marine diagenesis. In accordance to the geochemical model proposed by Odin and Matter (1981), Fe-rich smectite were initially precipitated in micropores of substrate sediments and then evolved through progressive incorporations of potassium element that produced micaceous glauconite minerals. Cloud (1955) advocated that K- poor, iron-enriched muds or micaeous minerals are considered the starting materials for glauconite formation. Alternatively, Pryor (1975) proposed a biogenic origin for glauconite through glauconitization of precursor fecal pellets in a shallow-marine environment. Nevertheless, the studied glauconitic sandy shale sediments were subjected latter to pedogenic modifications because of subaerial exposure that resulted into some pedogenic overprints (e.g., color mottling, desiccation mud-cracks, clay illuviation, glossifungites bioturbation and rootlets) (Figures 5G, H). A similar case of pedogenesis is also documented in the lacustrine carbonates of the El-Ris Formation (Figure 5I).

3.4. Transgressive–regressive (T–R) sequence stratigraphy

By applying the concept of transgressive–regressive (T–R) sequence stratigraphy proposed by Embry and Johannessen (1992), the studied Eocene–Oligocene sequence consists of two main systems tracts: a transgressive systems tract (TST) at the base and a regressive systems tract (RST) at the top. This sequence is bounded at its base and top by significant subaerial unconformities (maximum regressive surfaces; MRS). In this (T–R) sequence, all genetically-linked lithofacies packages lying in-between the basal subaerial unconformity (SB1) and the upward maximum flooding surface (mfs) are considered to be a transgressive systems tract (TST), whereas the regressive systems tract (RST) comprises all lithofacies developed from the onset to the end of regression, in other words, those facies deposited between the maximum flooding surface (MFS) and the subaerial unconformity (maximum regressive surface–MRS) at the top (Figure 6). Correspondingly, the transgressive systems tract (TST) in the studied sequence is composed of the shallow subtidal flat (FA1), coastal lagoonal (FA2) and open lagoon–reefal (FA4) facies associations dominating the Naqb, Qazzun and the Lower Hamra rock units, whereas the regressive systems tract (RST) consists of the highst shoreline representing both the glauconitic sandy shale facies and limestone interbeds of the Upper Hamra Member, lowstand fluvial sstones (FA5) of the Radwan Formation and lowstand lacustrine carbonates (FA6) of the El-Ris Formation (Figure 6). Again, the systems tract of the El-Hamra Formation is believed to represent a continuous shallowing-up depositional environment. Upward changes in glaucony facies maturity from high to low substantiate the upwardly increase of the regressive systems tract (RST) dominated over the area during the Bartonian–Priabonian transition (Mesaed and Suror, 1999, 2000; El Habaak et al., 2016). This regressive phase was terminated in the major disconformity at the end of the time of the El-Hamra deposition and prior to the laid down of the Oligocene Radwan sandstone.

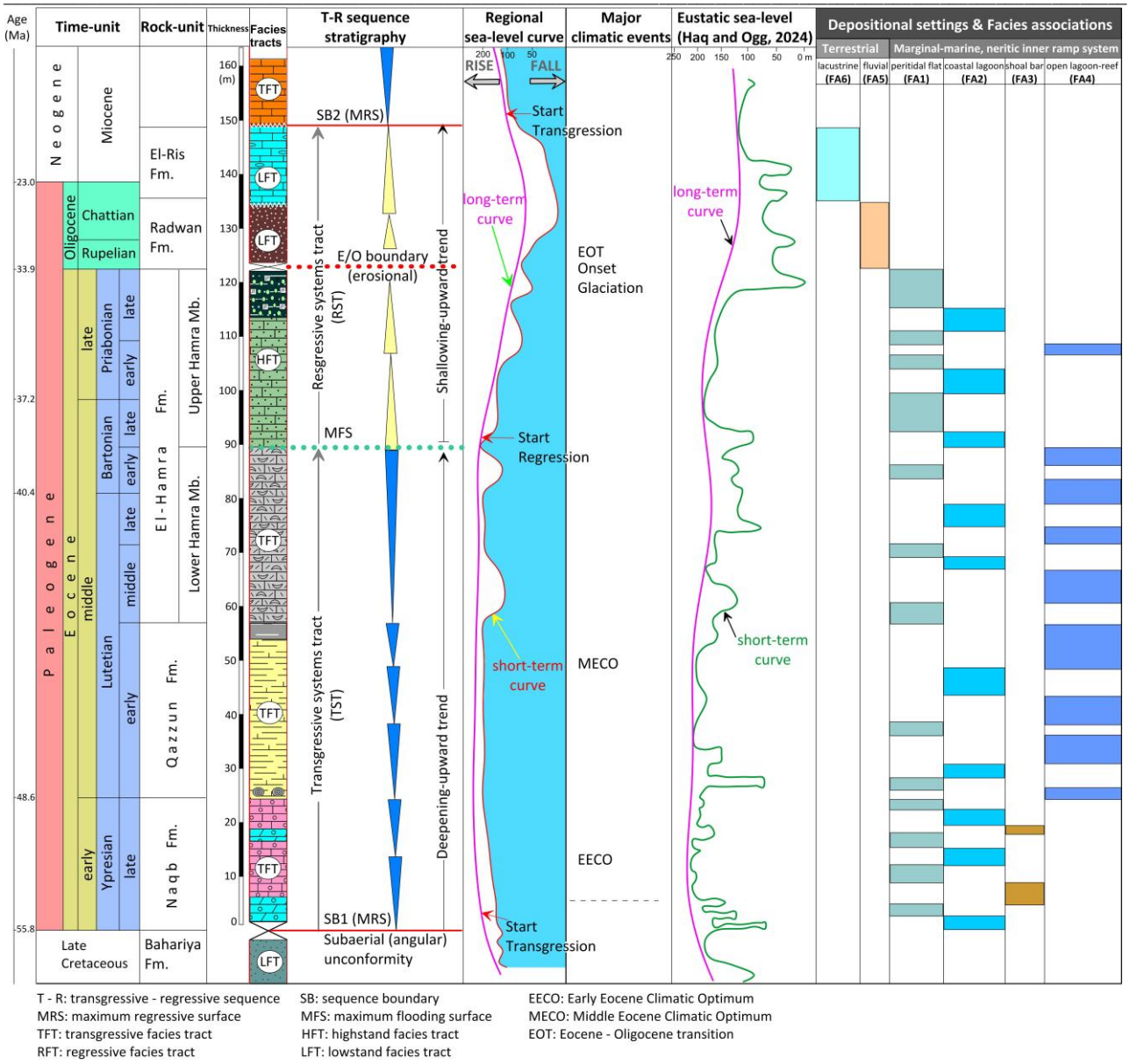

Figure 6. Chronostratigraphic chart highlighting the main sequence statigraphic elements, facies tracts and facies associations distinguished in the studied Eocene–Oligocene rocks (Ayoub et al., 2025a, b), as well as the hypothetical regional long-term sea-level curve compared with the global eustatic sea-level curve of Haq and Ogg (2004)

The change in depositional regime from transgressive to regressive (shallowing-upward) trend of the studied Eocene–Oligocene sequence was produced mainly in response to the progressive decrease in accommodation space and the increase of sediment accumulation, which are mostly attributed to the climatic change from the warm "greenhouse" state in the late Eocene to the "icehouse" conditions in the earliest Oligocene (Zachos et al., 1996), in addition to the non-negligible role of regional geotectonics on accommodation-to-sediment supply rates.

4. Discussion

4.1. Regional versus eustatic sea-level fluctuations

The stratigraphic relationship between the different facies associations identified in the studied Eocene–Oligocene rocks, in addition to the (T–R) sequence stratigraphic interpretations, has enabled the reconstruction of the regional changes in sea-level position during the Paleogene. Sea-level began to rise with the advent of the early Eocene and remained high throughout the entire middle Eocene, reaching its acme during the early Bartonian when the maximum flooding surface

(MFS) defined the change in depositional trend from a transgressive systems tract (TST) to a regressive systems tract (RST). A gradual shoreline regression began in the late Bartonian and continued during the Priabonian but with several short-term marine incursions. Sea-level falling reached its maximum in the late Oligocene when continental conditions prevailed in northern Egypt in general and the study area in particular (unconformities and discontinuities were also recorded from adjacent areas, e.g., Guiraud et al., 2005). This shift in sea-level marked the northern African margin, i.e. the passive margin of the southern Mediterranean platforms including Libya, Tunisia, Algeria and Morocco (Assal et al., 2024). Furthermore, it can be compared with other Mediterranean sectors located in its northern margins (Höntzsch et al., 2013). For example, the early–late Eocene successions deposited in inner and mid-ramp environments displaying a shallowing-upward (regression) trend into more restricted marine and terrestrial environments have been documented from southern Spain (Martín-Martín et al., 2020), southern Turkey (Önal and Kaya, 2007; Boulton, 2009), south-western France (Courme-Rault and Dubar, 2011) and Greece (Maravelis and Zelilidis, 2011).

The hypothetical regional sea-level curve established in the Bahariya study area can be compared with the already existed eustatic sea-level curves. Overall, the long-term regional sea-level matches well with the eustatic sea-level curves recently established by Haq and Ogg (2024) and Miller et al. (2024), indicating the presumed eustatic control on Paleogene sedimentation in the study area. The Ypresian–Lutetian–early Bartonian sea-level rise established in the study area is consistent with the global sea-level curve of Haq and Ogg (2024), which shows that the early–middle Eocene global eustatic sea-level oscillated, and started to fall towards the latest Eocene–Oligocene transition. A closure of the Tethyan Ocean took place in the late Eocene and was completed in the late Oligocene, accompanied by a significant drop of sea-level due to the onset of major accretion of ice-sheets on Antarctica (Haq and Al-Qahtani, 2005). Hence, the late Eocene in the study area witnessed a remarkable facies change from carbonate-dominated facies of the Qazzun Formation and the Lower Hamra Member (Lutetian–Bartonian) into siliciclastic-dominated facies with minor carbonate intercalations of the Upper Hamra Member (Priabonian), denoting to the lowstand sea-level position and change in the mode of deposition from the middle Eocene to the late Eocene. It appears therefore that a shallowing of the sea occurred gradually during the deposition of the El-Hamra Formation. The well-developed glaucony overburden deposits associated with pedogenic features (color mottiling, root traces and bioturbation), gypsum and caliche spots characterizing the topmost part of the Upper Hamra Member (Priabonian) provides a solid evidence of the marine regression off the area under consideration by the end of the Eocene, in response to the regional and eustatic sea-level drop (El Habaak et al., 2016).

4.2. Regional tectonics

The changes in the rate of tectonic subsidence in a basin or rate of uplift in the sediment source area largely control the ratio of sediment supply to accommodation space, which is responsible for sea transgression and regression (Emery and Myers, 1996). Siliciclastic supply into the shallow carbonate platforms might be a response to source-terrain tectonism (Osleger and Montanez, 1996). In the Bahariya region, the high topographic landmasses and many high structural fault-blocks induced by tectonic uplift of the Bahariya Swell and the Red Sea basement mountains in the east have resulted in increasing rates of physical and chemical weathering and, in turn, increasing amount of sediment input into the Bahariya basin, which led to a gradual sea regression to the north from the middle Eocene up to the late Eocene–Oligocene transition.

4.3. Palaeoclimate

The Eocene–Oligocene in the Bahariya region records a major transition from shallow-marine Eocene strata to unconformably overlying Oligocene nonmarine sandstone/lacustrine carbonate beds in response to the greenhouse-to-icehouse transition. This Eocene/Oligocene unconformity is represented by a condensed shallow-marine glauconitic-phosphatic-gypseous sandy shale section dominating the upper part of the Upper Hamra Member (Priabonian), followed upward by a red

sandstone paleosol horizon, which gives evidence of subaerial exposure, and topped then by fluviatile sandstone of the early Oligocene Radwan Formation and lacustrine carbonate beds of the El-Ris Formation, respectively. In the Teetotum Hill section, the lacustrine carbonate beds of the El-Ris Formation overlie disconformably the upper Hamra Member where the lower Oligocene Radwan sandstone is entirely missing. Besides, the Eocene carbonate platforms developed throughout the Mediterranean shelf regions were dominated by benthic foraminiferal and macrofunal contents, which favoured tropical and subtropical epipelagic shallow-marine, tidal, restricted lagoonal, reefal environments (BouDagher-Fadel and Price, 2013; Zoeram et al., 2015). Zobaa et al. (2015) provides palynological evidence for epicontinental dry subtropical to temperate climatic conditions during the deposition of the Eocene sediments along the southeastern Mediterranean regions.

5. Conclusion

The Eocene–Oligocene rocks in northern Bahariya Depression, Egypt, have been analyzed for their sedimentary facies, diagenetic features, paleoecology, and transgressive-regressive sequence stratigraphy. The main conclusions of this study are:

1) The Eocene rocks described in the study area constitute from base to top, the Naqb, Qazzun and El-Hamra formations, overlain by the Oligocene Radwan and/or El-Ris formations. Five distinctive macrofaunal assemblages were identified from the Eocene strata and interpreted ecologically.

2) Six depositional facies associations were discriminated in the studied Eocene–Oligocene rocks, which correspond to a range of depositional environments, from marginal marine to fluvial lacustrine settings.

3) The diagenetic features recorded in the examined rocks were resulted mostly from compaction, cementation, micritization, replacement (including dolomitization, silicification and iron replacement), dissolution and glauconitization.

4) The studied Eocene–Oligocene succession consists entirely of a transgressive–regressive (T–R) depositional sequence comprising two main facies tracts: the transgressive facies tract (TFT) regressive facies tract (RFT). This depositional sequence is bounded at its base and top by two sequence boundaries (SB1 and SB2, respectively). The shallowing-upward depositional trend (regression) of the studied Eocene–Oligocene sequence was formed in response to a progressive sea-level fall, which was mainly controlled by a palaeoclimate that abruptly cooled toward the Eocene–Oligocene transition (EOT), alongside with the non-negligible role of regional tectonics.

6. Supplementary Materials. There are no supplementary materials.

7. Author Contributions

Fieldwork, writing - original draft; methodology and lab investigation - N.A.; supervision, review – S.A.; fieldwork, supervision – R.O.; supervision – M.H.; conceptualization, data acquisition, fieldwork, methodology, formal analysis, supervision, writing–review and editing – E.S.

8. Author Information

Ayoub, Nada A. – researcher, Benha University, Farid Nada Street 15, Benha, Egypt, 13518; n.ayoub58969@fsc.bu.edu.eg, https://orcid.org/0009-0007-7322-3239

Ahmed, Sayed M. – Professor, Benha University, Farid Nada Street 15, Benha, Egypt, 13518; sayed.ahmed@fsc.bu.edu.eg, https://orcid.org/0000-0002-8699-5699

Osman, Rifaat A. – Professor, Benha University, Farid Nada Street 15, Benha, Egypt, 13518; r.othman@fsc.bu.edu.eg, https://orcid.org/0009-0001-7559-3379

Hassan, Mervat S. – Professor, Central Metallurgical Research Development Institute, 1, Elfelezat Street, El-Tebbin, Cairo, Egypt, 11912; mervat_hassan45@yahoo.com, https://orcid.org/0000-0002-7300-303X

Sallam, Emad S. – Professor, Benha University, Farid Nada Street 15, Benha, Egypt, 13518; emad.salam@fsc.bu.edu.eg, https://orcid.org/0000-0002-1629-5734

9. Funding: This research received no external funding.

10. Acknowledgements: The authors gratefully thank the journal editor and the both anonymous reviewers for their support.

11. Conflicts of Interest: The authors declare no conflict of interests.

12. References

1. Adams, J. E., & Rhodes, M. L. (1960). Dolomitization by seepage refluxion. *Bull. Am. Ass. Petrol. Geol*., 44, 1912-1920.
2. Afify, A. M., Serra Kiel, J., Sanz-Montero, M. E., Calvo, J. P., & Sallam, E. S. (2016). Nummulite biostratigraphy of the Eocene succession in the Bahariya Depression, Egypt: implications for timing of iron mineralization. *Journal of African Earth Sciences*, 120, 44-55. http://dx.doi.org/10.1016/j.jafrearsci.2016.04.016
3. Al-Dhwadi, Z., & Sallam, E. S. (2019). Spheroidal "Cannonballs" calcite-cemented concretions from the Faiyum Bahariya depressions, Egypt: evidence of differential erosion by s storms. *Internatioal Journal of Earth Sciences*, 108, 2291–2293. https://doi.org/10.1007/s00531-019-01753-3
4. Amorosi, A. (1995). Glaucony sequence stratigraphy: A conceptual framework of distribution in siliciclastic sequences. *J. Sediment. Res.*, 65, 419–425.
5. Assal, E. M., Wanas, H. A., & Abou Awad, H. A. (2024). The Middle-Upper Eocene in the Northern Plateau of the Bahariya Depression, Western Desert (Egypt) correlation with other Tethyan sectors. *Marine Petroleum Geology*, 161, 106705.
6. Attia, M. I. (1950). The geology of the iron-ore deposits of Egypt. *Geological Survey of Egypt*, 7, 34.
7. Ayoub, N. A., Ahmed, S. M., Osman, R. A., Hassan, M. S., & Sallam, E. S. (2025a). Facies evolution of the Eocene-Oligocene succession in Northern Bahariya Depression (Western Desert, Egypt): depositional controls, palaeoenvironments, palaeobiogeography. *Journal of Sedimentary Environments*, 10, 947-992. https://doi.org/10.1007/s43217-025-00263-4
8. Ayoub, N. A., Ahmed, S. M., Osman, R. A., Hassan, M. S., & Sallam, E. S. (2025b). Palaeoenvironments and palaeobiogeographical distribution of the Eocene larger benthic foraminifera and macrofaunal associations in the northern plateau of the Bahariya Depression, Western Desert, Egypt. *Benha Journal of Applied Sciences*, 10(2), 91-109.
9. Baioumy, H. M., & Hassan, M. S. (2004). Authigenic halloysite from El Gedida iron ores, Bahariya Oasis, Egypt: characterization origin. *Clay Minerals*, 39, 207–217.
10. Baioumy, H. M., Mohamed Z. Khedr, M. Z., & Ahmed, A. H. (2013). Mineralogy, geochemistry origin of Mn in the high-Mn iron ores, Bahariya Oasis, Egypt. *Ore Geology Reviews*, 53, 63–76.
11. Ball, J., & Beadnell, H. J. L. (1903). *Bahariya Oasis: its topography geology*. Egypt Surv. Dept., Egypt, 84.
12. Basta, E., & Amer, H. (1969). El Gedida iron ores their origin, Bahariya Oases, Egypt. *Economic Geology*, 64, 424–444.
13. Bell, D. L., & Goodell, H. G. (1967). A comprehensive study of glauconite the associated clay fraction in modern marine sediments. *Sedimentology*, 9, 169-202.
14. Blatt, H., Middleton, G. V., & Murray, R. C. (1980). Origin of Sedimentary Rocks. *Prentica-Hall, New Jersey*, 634.
15. Boukhary, M., Hussein-Kamel, Y., Abdelmalik, W., & Besada, M. (2011). Ypresian nummulites from the Nile Valley the Western Desert of Egypt: their systematic biostratigraphic significance. *Micropaleontology*, 571, 1-35.

16. Catuneanu, O. (2006). *Principles of Sequence Stratigraphy*. Elsevier (Amsterdam), 386 pp.
17. Catuneanu, O., Khalifa, M. A., & Wanas, H. A. (2006). Sequence stratigraphy of the Lower Cenomanian Bahariya Formation, Bahariya Oasis, Western Desert, Egypt. *Sedimentary Geology*, 190, 121–137.
18. Catuneanu, O., Galloway, W. E., Kendall, Ch. G. St. C., Miall, A. D., Posamentier, H. W., Strasser, A., & Tucker, M. T. (2011). Sequence stratigraphy: Methodology Nomenclature. *Newsletters on Stratigraphy*, Stuttgart, 44/3, 173–245.
19. Cloud, P. E. (1955). Physical limits of glauconite formation. *AAPG Bulletin*, 39, 484-492.
20. Dabous, A. A. (2002). Uranium isotopic evidence for the origin of the Bahariya iron deposits, Egypt. *Ore Geology Reviews*, 19, 165–186.
21. Dickson, J. A. D. (1965). A modified staining technique for carbonates in thin section. *Nature*, 205, 587.
22. Duff, P. McL. D., Hallam, A., & Walton, E. K. (1967). *Cyclic sedimentation*. Elsevier (Amsterdam), 280 pp.
23. Dunham, R. J. (1962). Classification of carbonate rocks according to depositional texture. In: Ham, W. E. (Ed.) Classification of carbonate rocks. *Tulsa, Okla. A.A.P.G. Memoirs*, 1, 108–121.
24. El Akkad, S., & Issawi, B. (1963). Geology iron ore deposits of the Bahariya Oasis: *Geological Survey Mineral Research Department*, 18, 301.
25. El Aref, M. M., & Lotfy, Z. H. (1985). Genetic karst significance of the iron ore deposits of El Bahariya Oasis, Western Desert, Egypt. *Annals Geological Survey of Egypt*, 15, 1–30.
26. El Aref, M. M., Mesaed, A. A., Khalil, M. A., & Salama, W. S. (2006). Stratigraphic setting, facies analyses depositional environments of the Eocene ironstones of Gabal Ghorabi mine area, El Bahariya Depression, Western Desert, Egypt. *Egyptian Journal of Geology*, 50, 29–57.
27. El Bassyony, A. A. (1980). The discovery of El Gedida iron ores their origin, Bahariya Oases, Western Desert, Egypt. *Journal of the Geological Society of Iraq*, 13, 119-130.
28. El Habaak, G., Askalany, M., Galal, M., & Abdel-Hakeem, M. (2016). Upper Eocene glauconites from the Bahariya Depression: An evidence for the marine regression in Egypt. *Journal of African Earth Sciences,* 117, 1-11.
29. El Sharkawi, M. A., Higazi, M. M., & Khalil, N. A. (1984). Three genetic iron ore dikes of iron ores at El Gedida mine, Western Desert, Egypt. *Geological Society of Egypt, 21st Annual Meeting*, Cairo, Egypt, p. 68.
30. El Shazly, E. M. (1962). Report on the results of drilling in the iron ore deposit of Gebel Ghorabi, Bahariya Oasis, Western Desert. *Egypt Geol. Surv.,* 17, 1–25.
31. Embry, A., & Johannessen, E. (1992). T-R sequence stratigraphy, facies analysis reservoir distribution in the uppermost Triassic-Lower Jurassic succession, western Sverdrup Basin, Arctic Canada: in T. Vorren et al., eds., Arctic Geology Petroleum Potential: *Norwegian Petroleum Society Special Publication,* 2, 121-146.
32. Eugster, H. P. (1969). Inorganic bedded cherts from the Magadi area, Kenya. *Contr. Mineral. Petrol.,* 22, 1-31.
33. Fischer, A. G., Honjo, S., & Garrison, R. E. (1967). Electron micrographs of limestones their nannofossils. *Princeton Monogr. Geol. Paleont.,* 1, 141.
34. Flügel, E. (2004). *Microfacies of carbonate rocks: Analysis, Interpretation Application*. Springer Berlin Heidelber (New York), 976 pp.
35. Flügel, E. (2010). Microfacies of Carbonate Rocks: Analysis, Interpretation Application. *Springer Verlag, New York*, 996 pp.
36. Folk, R. L. (1962). Spectral subdivision of limestone types, In: Ham, W. E. (Ed.) Classification of carbonate rocks - a symposium. *AAPG. Mem.,* 1, 62-84.
37. Folk, R. L. (1974). The nature of crystalline calcium carbonate, effect of magnesium content salinity. *Journal of Sedimentary Petrology*, 44, 40-53.

38. Friedman, G. M., & Sers, J. E. (1978). *Principles of Sedimentology*. John Wiley, New York, 792 pp.
39. Gheith, M. A. (1955). *Classification Review of Iron Ore Deposits*. Symposium of Applied Geology of Near East. UNESCO, Ankara, 106–113.
40. Haq, B. U., & Ogg., J. G. (2024). Retraversing the highs and lows of Cenozoic sea levels. *GSA Today*. https://doi.org/10.1130/GSATG593A.1
41. Heckel, P. H. (1972). Recognition of ancient shallow marine evironments. In: J. K. Rigby, W. K. Hamblin (Eds.), *Recognition of Ancient Sedimentary Environments*, Spec. Publ. Soc. econ. Paleont. Miner., Tulsa (16, pp. 226-296).
42. Heckel, P. H. (1974). Carbonate buildups in the geologic record: a review. In: L. F. Laporte (Eds.), *Reefs in Time Space*, Spec. Publ. Soc. econ. Paleont. Miner., Tulsa (18, pp. 90-154).
43. Keheila, E. A., & El-Ayyat, A. M. (1990). Lower Eocene carbonate facies, environments sedimentary cycles in Upper Egypt: evidence for global sea-level changes. *Palaeogeography Palaeoclimatology Palaeoecol*ogy, 81, 333–347.
44. Keheila, E. A., & El-Ayyat, A. M. (1992). Silicification dolomitization of the Lower Eocene carbonates in the Eastern Desert between Sohag Qena, Egypt. *Journal of African Earth Sciences*, 14, 341–349.
45. Khalifa, M. A., & Mashaal, N. M. (2023). Facies framework depositional setting of the Middle-Upper Eocene Hamra Formation, north of Bahariya Oasis, Western Desert, Egypt. *Arabian Journal of Geosciences*, 16, 207.
46. Knauth, L. P. (1979). A model for the origin of chert in limestone. *Geology*, 7(6), 274-277.
47. Laschet, C. (1984). On the origin of cherts. *Facies*, 10, 257-289.
48. Longman, M. W. (1977). Factors controlling the formation of microspar in the Bromide Formation. *Journal of Sedimentarty Petrology*, 47, 347-350.
49. MacRae, S. G. (1972). Glauconite. *Earth-Science Reviews*, 8, 397-440.
50. McBride, E. F. (1989). Quartz cement in sstones: A review. *Earth-Science Reviews*, 26, 69-112.
51. Mesaed, A. A., & Suror, A. A. (1999). Mineralogy geochemistry of the Bartonian stratabound diagenetic lateritic glauconitic ironstones of El-Gideda mine, Bahariya Oasis, Egypt. *2nd International Conference on the Geology of the Arab World, Cairo Univ., Egypt*, 1, 509-540.
52. Mesaed, A. A., & Suror, A. A. (2000). Mineral chemistry mechanism of formation of the Bartonian glaucony of El Gedida mine, El Bahariya Oasis, Egypt. *Egyptian Mineralogist*, 12, 1-28.
53. Moustafa, A. R., Saoudi, A., Moubasher, A., Ibrahim, I. M., Molokhia, H., & Schwartz, B. (2003). Structural setting tectonic evolution of the Bahariya Depression, Western Desert, Egypt. *GeoArabia*, 8 (1), 91-124.
54. Nakhla, F. M. (1961). The iron ore deposits of El-Bahariya Oasis, Egypt. *Economic Geology*, 56, 1103–1111.
55. Odin, G. S., & Fullagar, P.D. (1988). Geological Significance of the Glaucony Facies. In Green Marine Clays: Oolitic Ironstone Facies, Verdine Facies, Glaucony Facies Celadonite-Bearing Rock Facies - A Comparative Study. *Developments in Sedimentology*, 45, 295–332.
56. Odin, G. S., & Matter, A. (1981). De glauconiarum origine. *Sedimentology*, 28, 611–641.
57. Peterson, M. N. A., & von der Borch, C. C. (1965). Chert: modern inorganic deposition in a carbonate-precipitating locality. *Science*, 149, 1501-1503.
58. Pettijohn, F. J., Potter, P. E., & Siever, R. (1973). *Sand and Sandstone*. Springer-Verlag New York, Heidelberg, Berlin, 618 pp.
59. Plyusnina, E. E., Sallam, E. S., & Ruban, D. A. (2016). Geological heritage of the Bahariya Farafra oases, the central Western Desert, Egypt. *Journal of African Earth Sciences*, 116, 151-159.
60. Pryor, W. A. (1975). Biogenic sedimentation alteration of argillaceous sediments in shallow marine environments. *Bulletin Geological Society of America*, 86, 1244–1254.
61. Said, R. (1962). *The geology of Egypt*. Elsevier Publ. Co. Amesterdam New York, 377 pp.

62. Said, R. & Issawi, B. (1964). Geology of northern plateau, Bahariya oasis, Egypt. *Geological Survey of Egypt*, 29, 41.
63. Salama, W., El Aref, M. M., & Gaupp, R. (2015). Spectroscopic characterization of iron ores formed in different geological environments using FTIR, XPS, Mössbauer spectroscopy thermoanalyses. *Spectrochimica Acta Part A: Molecular Biomolecular Spectroscopy*, 136, 1816–1826.
64. Sallam, E. S., & Ruban, D. A. (2019). Ancient tufa semi-detached megaclasts from Egypt: evidence for sedimentary rock classification development. *Internatioal Journal of Earth Sciences*, 108(5), 1615–1616.
65. Sallam, E. S., Issawi, B., & Osman, R. (2015a). Stratigraphy, facies, depositional environments of the Paleogene sediments in Cairo-Suez district, Egypt. *Arabian Journal of Geosciences*, 8 (4), 1939–1964.
66. Sallam, E. S., Wanas, H. A., & Osman, R. (2015b). Stratigraphy, facies analysis sequence stratigraphy of the Eocene succession in the Shabrawet area (north Eastern Desert, Egypt): An example for a tectonically influenced inner ramp carbonate platform. *Arabian Journal of Geosciences*, 8 (12), 10433-10458.
67. Sallam, E. S., Ruban, D. A., & Van Loon, A. J. (2022). Lagoonal carbonate deposition preceding rifting-related uplift: evidence from the Bartonian–Priabonian (Eocene) in the northwestern Gulf of Suez (Egypt). *Journal of Palaeogeography*, 11 (1), 8-30 (00254).
68. Sallam, E. S., Erdem, N. Ö., Sinanoğlu, D., & Ruban, D. A. (2018). Mid-Eocene (Bartonian) larger benthic foraminifera from southeastern Turkey northeastern Egypt: New evidence for the palaeobiogeography of the Tethyan carbonate platforms. *Journal of African Earth Sciences*, 141, 70-85.
69. Serra-Kiel, J., Hottinger, L., Caus, E., Drobne, K., Ferrandez, C., Jauhri, A. K., Less, G., Pavlovec, R., Pignatti, J., Samso, J. M., Schaub, H., Sirel, E., Strougo, A., Tambareau, Y., Tosquella, J., & Zakrevskaya, E. (1998). Larger foraminiferal biostratigraphy of the Tethyan Paleocene and Eocene. *Bull. Soci. Geol. Fr.*, 169(2), 281-299.
70. Sinanoğlu, D., Erdem, N. Ö., & Sallam, E. S. (2018, Aprile 4-13). *Bartonian benthic foraminifera: Examples from the Arabian North African carbonate platforms*. 20th EGU General Assembly, EGU2018, Vienna, Austria, 6500 p.
71. Tanner, L. H., & Khalifa, M. A. (2010). Origin of ferricretes in fluvial-marine deposits of the Lower Cenomanian Bahariya Formation, Bahariya Oasis, Western Desert, Egypt. *Journal of African Earth Sciences*, 56, 179-189.
72. Tosson, S., & Saad, N. A. (1974). Genetic studies of El-Bahariya iron ore deposits, Western Desert, Egypt. *Neues Jb. Miner. Abh.*, 121, 317–393.
73. Tucker, M. E. (1981). *Sedimentary Petrology: An Introduction*. Blackwell Scientific Publications. 2nd edition, Oxford, London, Geoscience texts, 3, 252 pp.
74. Tucker, M. E., & Wright, V. P. (1990). *Carbonate Sedimentology*. Blackwell Science, Oxford, 482 pp.
75. Walker, R. G. (1979). Facies models. *Geoscience Canada*, 211.
76. Wanas, H. A., Armenteros, I., Recio, C., Sallam, E. S., & Nieto, C. E. (2023). Distal fluvial to lacustrine/palustrine carbonate facies of the El-Ris Formation (Late Miocene?) at the Bahariya Depression, Western Desert, Egypt: Depositional model controls. *Journal of African Earth Sciences*, 205, 104993.
77. Waugh, B. (1970). Petrology, provenance silica diagenesis of the Penrith Sstone (Lower Permian) of northwest Engl. *Journal of Sedimentary Petrology*, 40, 1226-1240.
78. Wilson, J. L. (1975). *Carbonate Facies in Geologic History*. New York (Springer), 471 pp.
79. Zachos, J. C., Quinn, T. M., & Salamy, K. A. (1996). High-resolution (104 yr) deep-sea foraminiferal stable isotope records of the Eocene-Oligocene climate transition. *Paleoceanography*, 11, 251–266.

80. Zobaa, M. K., Sallam, E. S., & Oboh-Ikuenobe, F. E. (2015). Palynological evidence for epicontinental dry subtropical to temperate climatic conditions during the Eocene in the southeast Mediterranean. *Geological Society of America, Abstracts and Program,* 47(7), 142.

Эоцен–Олигоцендік тізбектің интеграциялық фациялық талдауы, палеоэкологиясы және диагенетикалық эволюциясы, Солтүстік Бахария ойысы, Мысыр: секвенциялық стратиграфиялық көзқарастар

Nada A. Ayoub, Sayed M. Ahmed, Rifaat A. Osman, Mervat S. Hassan, Emad S. Sallam

Аңдатпа. Бұл зерттеу Солтүстік Бахария ойысы, Батыс шөл, Мысырда ашылған Эоцен–Олигоценге жататын тізбектің седименттік фацияларын, палеоэкологиялық, секвенциялық және диагенетикалық ерекшеліктерін сипаттайды. Бұл Эоцен–Олигоцен тізбек бес стратиграфиялық бірліктен тұрады: негізінен жоғарыға қарай Naqb (ерте Эоцен), Qazzun (орта Эоцен) және El-Hamra (орта–кейінгі Эоцен) формациялары, содан кейін Radwan (ерте Олигоцен) және El-Ris (кейінгі Олигоцен–Миоцен) формациялары орналасқан. Зерттелген эоцендік тау жыныстарынан бірнеше әртүрлі ірі бентикалық фораминифера және макрофауналық қауымдастықтар анықталып, экологиялық тұрғыда талданды. Лито-, био- және микрофациялық талдаулар нәтижесінде алты негізгі фациялық ассоциация анықталды, олар эоцендік жыныстарда перитидальды жазықтардан шектелген және сыртқы лагуналарға, рифтік ортаға дейінгі ауқымды көрсетсе, олигоцендік жыныстарда өзендік және беткей көлдік жерүсті ортаға сәйкес келеді. Зерттелген жыныстардағы ең жиі кездесетін диагенетикалық ерекшеліктер цементация, доломитизация, силиктизация, глауконитизация және темірмен алмастырудан туындаған болуы мүмкін.
Зерттелген Эоцен–Олигоцен тізбек екі негізгі жүйелік трактіден тұрады: төменгі жағында трангрессивтік жүйелік тракт, ал жоғары жағында регрессивтік жүйелік тракт орналасқан. Седименттік үрдістің трангрессивтік режимнен регрессивтік режимге ауысуы негізінен орналастыру орнының азаюы мен седименттің келу көлемінің артуына байланысты дамыған.

Түйін сөздер: фациялық талдау; диагенез; тізбекті стратиграфия; Эоцен; Олигоцен; Бахария ойпаты.

Интегрированный анализ фаций, палеоэкология и диагенетическая эволюция Эоцен–Олигоценовой толщи, северная часть впадины Бахария, Египет: последовательностные стратиграфические перспективы

Nada A. Ayoub, Sayed M. Ahmed, Rifaat A. Osman, Mervat S. Hassan, Emad S. Sallam

Аннотация. Это исследование описывает осадочные фации, палеоэкологические, последовательностные и диагенетические особенности Эоцен–Олигоценовой толщи, обнаженной в северной части впадины Бахария, Западная пустыня, Египет. Эта Эоцен–Олигоценовая толща состоит из пяти стратиграфических единиц: снизу вверх Naqb (ранний эоцен), Qazzun (средний Эоцен) и El-Hamra (средний–поздний Эоцен), за которыми следуют формации Radwan (ранний олигоцен) и El-Ris (поздний Олигоцен–Миоцен). Из изученных эоценовых пород было идентифицировано несколько различных сообществ крупных бентосных фораминифер и макрофауны, интерпретированных с экологической точки зрения. Анализ лито-, био- и микрофаций позволил выделить шесть основных фациальных ассоциаций, отражающих диапазон от перитидальных равнин до ограниченных и внешних лагун, рифовых сред эоценовых пород и речных и мелководных озерных наземных сред

олигоценовых пород. Наиболее часто встречающиеся диагенетические особенности в изученных породах, вероятно, связаны с цементацией, доломитизацией, силификацией, глауконитизацией и замещением железом.
Изученная Эоцен–Олигоценовая толща включает два основных системных тракта: трангрессивный системный тракт внизу, за которым вверх следует регрессивный системный тракт. Смена осадконакопления от трангрессивного к регрессивному режиму в основном развивалась в ответ на постепенное уменьшение пространства для осадконакопления и увеличения поступления осадков.

Ключевые слова: фациальный анализ; диагенез; последовательная стратиграфия; Эоцен; Олигоцен; впадина Бахария.